Title

Live Cell Lineage Tracing of Dormant Cancer Cells.

Journal

Advanced Healthcare Materials, 12(14)

Authors

Kim, Hyuna
Wirasaputra, Anna
Mohammadi, Farnaz
et al.

Publication Date

2023-06-01

DOI

10.1002/adhm.202202275

Peer reviewed

HHS Public Access

Author manuscript

Adv Healthc Mater. Author manuscript; available in PMC 2024 June 01.

Published in final edited form as:

Adv Healthc Mater. 2023 June ; 12(14): e2202275. doi:10.1002/adhm.202202275.

Live Cell Lineage Tracing of Dormant Cancer Cells

Hyuna Kim[1], **Anna Wirasaputra**[2], **Farnaz Mohammadi**[3], **Aritra Nath Kundu**[2], **Jennifer A.E. Esteves**[4], **Laura M. Heiser**[5], **Aaron S. Meyer**[3,6], **Shelly R. Peyton**[1,2,4,*]

[1]Molecular and Cell Biology Graduate Program, University of Massachusetts Amherst, USA

[2]Department of Chemical Engineering, University of Massachusetts Amherst, USA

[3]Department of Bioengineering, University of California, Los Angeles, USA

[4]Department of Biomedical Engineering, University of Massachusetts Amherst, USA

[5]Department of Biomedical Engineering, Knight Cancer Institute, Oregon Health & Science University, Portland, USA

[6]Jonsson Comprehensive Cancer Center, University of California, Los Angeles, USA

Abstract

Breast cancer is a leading cause of global cancer-related deaths, and metastasis is the overwhelming culprit of poor patient prognosis. The most nefarious aspect of metastasis is dormancy, a prolonged period between primary tumor resection and relapse. Current therapies are insufficient at killing dormant cells; thus, they can remain quiescent in the body for decades until eventually undergoing a phenotypic switch, resulting in metastases that are more adaptable and more drug resistant. Unfortunately, dormancy has few *in vitro* models, largely because lab-derived cell lines are highly proliferative. Existing models address tumor dormancy, not cellular dormancy, because tracking individual cells is technically challenging. To combat this problem, we adapted a live cell lineage approach to find and track individual dormant cells, distinguishing them from proliferative and dying cells over multiple days. We applied this approach across a range of different *in vitro* microenvironments. Our approach revealed that the proportion of cells that exhibited long-term quiescence was regulated by both cell intrinsic and extrinsic factors, with the most dormant cells found in 3D collagen gels. We envision that this approach will prove useful to biologists and bioengineers in the dormancy community to identify, quantify, and study dormant tumor cells.

Graphical Abstract

*corresponding author.

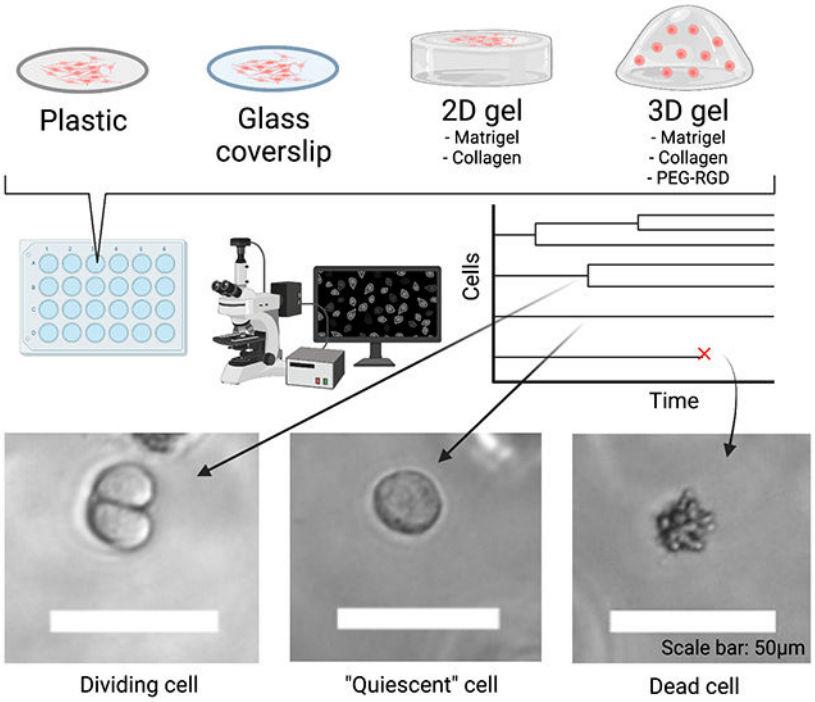

A live cell lineage approach was adapted to find and track individual dormant cells. This approach can be applied across a range of different *in vitro* microenvironments. This approach reveals that the proportion of cells that exhibited long-term quiescence was regulated by both cell intrinsic and extrinsic factors, with the most dormant cells found in 3D collagen gels.

Keywords

Breast cancer; biomaterials; collagen; Matrigel; poly(ethylene glycol) hydrogel

Introduction

2.3 million women worldwide were diagnosed with breast cancer in 2020, with approximately 685,000 reported deaths.[1,2] The 5-year and beyond survival rate varies based on region and breast cancer subtype, with 85-90% survival in high-income countries and 60% or lower in many developing countries.[3,4] It is important to note, however, that these statistics are associated with reporting disparity from lower-middle income areas.[5]

When breast cancer is at stage I or II, tumor growth is controllable with chemotherapy, surgery, and radiation, and 5-year survival rate is 90-100% in the United States.[6,7] However, when breast cancer metastasizes to other organs, the survival rate dramatically decreases to 22%.[8] Breast cancer commonly metastasizes to bone, lung, brain, and liver. Even after initially successful treatment, 13-30% of early-stage breast cancer patients develop cancer relapse in distant organs, most frequently in the bone.[9,10] This indicates that disseminated tumor cells (DTCs) can remain dormant for many years, even decades, before growing into a detectable, symptomatic tumor.[9,10] It is difficult to treat these dormant cells

as traditional chemotherapies target rapidly growing cells. Also, regardless of their cell cycle status, DTCs are actively protected by their microenvironment and vascular endothelium.[11]

Dormancy is categorized either as tumor mass dormancy or cellular dormancy. Tumor mass dormancy states that the rate of cancer cell proliferation in a bulk of tumor equals that of cell death.[12] Cellular dormancy is a result of an individual DTC temporarily exiting the cell cycle and remaining in a quiescent state, with the possibility that it can resume proliferation later.[12] Researchers have been studying the critical factors and the molecular mechanisms governing dormancy and subsequent relapse, but it is challenging to find and track individual DTCs that are both viable and dormant. For instance, immunohistochemistry (IHC) of fixed clinical and *in vivo* specimens can provide insight into localization of dormant or proliferating cells within the matrix by comparing the levels of Ki-67 expression.[13,14] However, IHC cannot determine if the observed non-proliferative cells are capable of eventual outgrowth, nor if the factors from their microenvironment would affect the outgrowth because the process is limited to fixed samples.

Moreover, most of the traditional *in vitro* models fail to capture the interactions between cancer cells and their microenvironment. Currently, the majority of dormancy models exist on 2D systems, mainly plastic or protein-treated coverslips due to ease of use and greater reproducibility. While it yields more consistent results, the differences between these 2D systems and native tissue present many limitations. One of the biggest differences involves tumor cell morphology and how a flat versus spherical geometry changes the adhesion of the cells to the extracellular matrix (ECM) and the drug efficacy of certain treatments. Thus, there is a greater push to develop novel 3D environments using either polyethylene glycol (PEG) or polyacrylamide, though less than 20% of papers reviewed from Micalet *et al.* contained these systems.[15] These 3D models are favored over the 2D systems as they mimic more accurate cell behavior in the body by providing similar mechanical and chemical properties of the body's premetastatic niches. The Kloxin lab created a bio-inspired 3D growing environment for predominantly ER+ cancer cells (T47D and BT474) to more accurately identify key differences in ECM compositions for late relapse events.[16] Similarly, the Slater lab pushed for tunable RGD hydrogels that allowed in-depth studies of dormancy reactivation by changing the chemical and mechanical properties and identifying phenotypic switches for encapsulated MDA-MB-231 cells.[17] Another example of showing the interactions between cancer cells and their microenvironment is work from the Ghajar lab, who, via intravital imaging, showed that certain microenvironments, like perivascular niches, protect DTCs from chemotherapy.[11] The overwhelming advantage of intravital imaging is the ability to watch DTCs in an *in vivo* context, but is expensive, difficult to learn, and is low throughput. We see intravital imaging as an excellent way to test specific hypotheses, but not well-suited for screening larger numbers of conditions. Creating *in vitro* approaches to observe cell quiescence and reactivation are sorely needed to better understand the factors that lead to relapse, such as that demonstrated here.

In order to track cell plasticity with greater accuracy, the Heiser lab developed a method to classify cells according to their heterogeneous phenotypes across lineages.[18] We adapted this model to create cell lineage trees and analyzed individual cell proliferation and death. This method can solve the problems that other commonly used cell proliferation assays

have. For example, the MTT assay is an endpoint assay, and it often overestimates cell viability.[19] Immunofluorescent staining, a commonly used method for assessing protein expressions, is also an endpoint assay which requires cell fixation. Live microscopy and manual tracking of cells through this lineage tracking allowed us to find and distinguish quiescent cells from proliferating and dying cells. We present this approach here, validated with established markers of cellular dormancy, to demonstrate the emergence of dormant populations across a variety of cell culture environments.

Results

IHC subtypes of breast cancer cell lines correlates with observed proliferation and dormancy rates

HCC1954 is a HER2 enriched (HER2+) ER− breast cancer cell line, which is a subtype correlated with more metastasis in the clinic, and more proliferative than luminal A type cell lines such as MCF7 (from Cellosaurus). We observed the HCC1954 cell lineage trees to have a higher distribution of cells proliferating twice or more than those in MCF7 (Figs. 1a–b, S1a–b), as expected. More than 50% of the randomly selected HCC1954 cells divided twice or more (Figs. 1a–b). According to Cellosaurus, a cell ancestry database, HCC1954 has a doubling time of 45 hours and MCF7 has a maximum doubling time of 80 hours, which further validates the difference in cell proliferation between the two cell lines. When comparing the cell lineage trees of HCC1954 and MCF7 cultured on tissue culture polystyrene (TCPS), there are a smaller number of non-dividing cells, illustrated as a single straight line across the graph, in HCC1954 than in MCF 7 (Figs. 1a–b, S1a–b). In this paper, we define the non-dividing live cells as “dormant” cells, as they don’t divide and don’t die but rather persist over the entire course of the experiment.

Dormant cell population increases on glass coverslips compared to that on TCPS

We tracked cells on glass substrates that were chemically functionalized with individual cell proteins or peptides, as we have described elsewhere.[20,21] Collagen and collagen-derived peptides (GFOGER) were chosen based on our prior work that demonstrated collagen I-functionalized surfaces as supporting cell entrance into dormancy *in vitro*.[22] Cell attachment was overall lower on these protein- and peptide-functionalized glass coverslips, and we also observed higher rates of cell death than those on TCPS (Figs. 1a–b, 1e–h). To ensure that the numbers of cells attached to the surfaces was equitable, we seeded cells at a higher density on protein- and peptide-functionalized surfaces. The number of dormant cells was higher on glass coverslips than on TCPS (p-value = 0.36, n = 3). Overall, the dormant cell population on both the rat tail collagen I functionalized and the collagen I peptide (GFOGER) functionalized coverslips had similar trends (Figs. 1f–h); though, the cells seeded on the GFOGER functionalized coverslips had a lower number of cells that divided twice or more than the cells seeded on the collagen I protein functionalized coverslips (Fig. 1h). Additionally, cells cultured on the protein- or peptide-functionalized coverslips had a higher portion of dormant cells while had lower cell death than the control, PBS-treated coverslips (Figs. 1e–h). Specifically, collagen I drove higher numbers of dormant cells compared to the PBS and GFOGER-treated coverslips (p-values of 0.044 and 0.19, respectively). Together, this tells us that collagen-functionalized glass coverslips

allow cells to undergo dormancy, and the form of collagen – either whole collagen protein or a part of the protein which is GFOGER peptide – does not have a significant effect on dormant cell population.

Higher proportions of dormant cells are found in 3D environments.

Matrigel and collagen gels are commonly used materials for cancer studies as collagen is the most abundant protein in human connective tissues, and Matrigel is extracellular matrix (ECM) extracted from Engelbreth-Holm-Swarm mouse tumors.[23] When MCF7 and HCC1954 cell lines were cultured on 2D Matrigel, both were less proliferative in comparison to TCPS (Figs. 1b, 2b, S1, S2). The HCC1954 line had a greater number of deaths over the course of the experiment for both serum-containing and serum-free media conditions (Fig. 2b). This suggests those cells have a greater sensitivity to serum deprivation, which we also observed in a previous dormancy study.[22] Additionally, both cell lines cultured on 2D Matrigel appeared to have lower proliferation than when cultured on TCPS, which could be due to the higher softness of Matrigel, which is known to influence cell proliferation rates.[24,25] However, the dormant cell population does not significantly change in both cell lines on 2D Matrigel compared to those on TCPS (Figs. 1a–b, 2b–c, S1, S2a–b). MCF7 cells showed less cell death on 2D Matrigel (Figs. 2c, S2a) while HCC1954 suffered more cell death (Figs. 2b, S2b). Also, there were more dormant MCF7 cells observed after 50 hours in culture (Figs. 2c, S2a) than HCC1954 (Figs. 2b, S2b), in both serum-containing and serum-free growth media conditions. Together, 2D Matrigel environment does not have a significant effect on dormant cell populations in both HCC1954 and MCF7, but the dormant cell population differs by cell line, which means the IHC subtypes of breast cancer cell lines play more significant role in dormancy than the 2D Matrigel environment itself does.

Significant differences in cell growth behavior, especially the dormant cell population, were observed when compared these cell lines on the same ECM protein in 2D versus 3D (p-value 0.002). HCC1954 cells were cultured on 2D collagen gels and in 3D collagen gels, and more than 50% cells were dormant in 3D collagen gel environment (Figs. 2d, S3b) while less than a quarter of the cells were dormant when cultured on a 2D collagen gel (Figs. 2a, S2c). Interestingly, about the same number of cells were dormant for 50 hours in both serum-containing and serum-free conditions in 3D collagen gels, but there were greater numbers of cells dying in the 3D collagen material than 2D (Figs. 2d, S3b). While the 3D collagen environment resulted in a higher number of dormant cells than 2D collagen gel environment, it showed the opposite trend in Matrigel. There were a greater number of dormant cells on 2D Matrigel (Figs. 2b, S2b) than in 3D Matrigel (Figs. 2e, S3a). Additionally, when comparing the matrix materials in the same dimension, 2D collagen gel vs. 2D Matrigel for example, the matrix material does not play a significant role in dormancy when it’s on 2D (Figs. 2a–b); however, when it’s in 3D, there was a significant difference in dormant cell population between cells in 3D collagen gels and those in 3D Matrigel. These results show that the types of matrix materials have a greater effect in 3D than on 2D. In HCC1954 cells, we observed higher proportions of dormant cells in 3D collagen compared to 3D Matrigel (p-value 0.0001 with FBS, p-value 0.0006 without FBS),

and MCF7 cells have a non-statistically significant similar trend (p-value 0.2 with FBS, p-value 0.8 without FBS) (Figs. 2f–g, S3c–d).

Immunofluorescence staining validates the cell lineage tree approach to identify dormant cells.

Two different mouse breast cancer cell lines from the same origin were used to validate if the cell lineage tree analysis is a viable method to use for dormancy study. D2A1 is a proliferative cell line and D2.0R is a dormant cell line.[26–29] Both cell lines showed high proliferation in serum containing medium in 3D Matrigel (Figs. 3a–b). Significant differences in proliferation (p-value 0.24) and dormancy (p-value 0.018) between these two cell lines was observed when they were cultured in serum-free media. D2.0R, the dormant cells, showed less cell death and more dormant phenotypes in serum-free environment than D2A1, the proliferative cells, and there were more non-dividing alive D2.0R cells when cultured in serum-free media than in serum-containing media (Figs. 3a–b). This result supports an earlier study that showed that serum deprivation forced cells into dormant-like state.[22]

Cells were immunofluorescently stained with Ki-67, ERK, p38 and DAPI to validate that the differences we saw in numbers of dormant cells using cell lineage tracking was reflected by the standard set of markers used to identify dormant cells. Dormant cells are distinguished by low Ki-67, low ERK, and high p38 expression.[30,31] Both Ki-67 and ERK expression were significantly lower in each cell line without FBS than with FBS, but there was no significant difference observed when comparing between the D2A1 and D2.0R in serum-containing media (Figs. 3c–d). There were relatively few dormant cells (ERK-low and p38-high) in serum-containing environments for both cell lines (Figs. 3c, 3e–f). D2.0R cells showed significantly lower ERK expression than the D2A1 cells when cultured in serum-free conditions (Figs. 3c–d). The D2.0R cells cultured in without serum in 3D Matrigel had the most cells that were positive for dormancy markers (low ERK and high p38) than any other conditions (Figs. 3c–f), validating our results from the cell lineage tree analyses.

TNBC cells did not show significant differences in dormant cell populations with or without serum in 3D environments

Breast cancer recurrence rates and regions vary depending on its molecular subtypes. For example, triple negative breast cancer (TNBC) accounts for 10-20% of all breast cancer cases, but it is highly aggressive and heterogeneous, and it has the highest recurrence rate in the first five years.[16,32] Although this is not a subtype that typically results in clinical dormancy, we wanted to see if this approach could in fact capture small numbers of cells that could be forced into a non-proliferative state and monitored. We performed experiments with two different human TNBC cell lines; MDA-MB-231s and HCC1143s. We cultured them in 3D collagen gels and Matrigel with or without serum. Unlike MDA-MB-231s on TCPS, which showed significant differences in non-dividing cell populations (p-value <0.0005), neither HCC1143 nor MDA-MB-231 cells were significantly different in the number of non-dividing cells in 3D Collagen or Matrigel (Figs. 4a–c, S4a–c). Regarding MDA-MB-231 cells, although the numbers of dormant cells were higher in serum-free

condition than in serum-containing condition in 3D Collagen (p-value 0.42) and Matrigel (p-value 0.16), they were not statistically significant (Figs. 4c). We also did not observe a difference when comparing between the 3D materials (p-value 0.76 for 3D Collagen vs. Matrigel with FBS, and p-value 1 without FBS).

Applications in 3D synthetic hydrogels

Several synthetic *in vitro* platforms have been developed to compete with naturally derived materials like collagen gel and Matrigel, as the synthetic materials enable more tunability and more precise control over its properties than protein-based hydrogels.[23] We cultured HCC1143, in 3D poly(ethylene glycol) (PEG) hydrogels containing widely used integrin-binding peptide sequence Arg-Gly-Asp (RGD) and partially crosslinked with a matrix metalloproteinase (MMP) sensitive peptide. Cells proliferated more in the degradable PEG-RGD hydrogels than in the non-degradable hydrogels (Fig. 4d). Less cell death and faster cell growth were achieved in growth media condition supplemented with epithelial growth factor (EGF) than in regular serum containing media, but the dormant cell population does not change significantly (p-value 1) upon EGF addition (Figs. 4d, S4d). This suggests that the addition of growth factors influences cell proliferation, but it does not play a significant role in dormant cell populations in 3D synthetic PEG-RGD hydrogels. The presence of MMP-degradable sites in the 3D synthetic environment resulted in fewer non-dividing cells, but this trend was not statistically significant (p-value 0.36 in 10% serum, and 0.64 in 10% serum + EGF).

Cell clonality differences in dormancy tracking

Thus far, all studies were performed on heterogeneous cell lines, where observations could be determined by both microenvironment and the genetic differences within these populations. Thus, we created cell subclones from the otherwise heterogeneous MDA-MB-231 cells, a triple negative breast cancer cell line,[33] and its cell subclones were cultured in PEG-RGD hydrogels of 2 kPa modulus with MMP-degradable sites. Although the subclones originated from the same cell line, their proliferation, death, and dormancy rates varied, demonstrating the power of cell intrinsic factors in driving dormancy and growth (Figs. 4e–f, S4e). Though, the differences across the cell subclones were not in statistically significance. This implies that differences observed across the unique cell lines we tested were much stronger than when comparing across available cell subclones within a single cell line. Together, these results conclude that the cell lineage tree analysis can be used to analyze growth behavior of cells of various subtypes on diverse culturing environment to track and identify individual dormant cells while keeping them alive.

Serum recovery triggers dormant cells to resume proliferation

Truly dormant cells should be able to re-stimulate proliferation under appropriate environmental contexts. Thus far, our data has shown only lack of proliferation over 50 hours of imaging, and these cells could be either dormant or senescent (permanently exiting the cell cycle). To distinguish between dormant and senescent cells, we re-introduced serum (10% FBS) to D2A1 and D2.0R cells cultured in 3D collagen and Matrigel, after a serum deprivation period, and continued imaging for an additional 48 hours (Fig. 5). A greater fraction of D2.0R cells resumed proliferation during serum recovery, compared to the D2A1

line when comparing across the same environment (p-value 0.3692 in collagen, 0.3618 in Matrigel). More strikingly, the dormant cell population varied significantly in D2.0R cell lines under different environmental conditions (collagen vs Matrigel, p-value 0.0060). This data shows that serum recovery triggers quiescent cells to re-proliferate, allowing us to distinguish dormant cells (Supplemental video S7) from possibly senescent cells (Supplemental video S8).

Discussion

Here we adapted a live cell tracking approach, where we can, in real time, with living cells, distinguish quickly between actively dividing cells, dying cells, and quiescent cells without the need for a fluorescent reporter. When combined with immunofluorescent staining at the end of the experiment, we can confirm which quiescent cells were in a dormant state using an accepted set of dormancy markers (Ki67-, ERK-low, and p38-high).[34,35] Combined with statistical analyses, information about these individual cells can go even further, revealing a rich data set where we can extract differences in both intrinsic and extrinsic regulators of proliferation vs. quiescence. By combining lineage tracing with control over tumor cell environments, we propose this as a method to carefully examine cellular dormancy over a near limitless extracellular parameter space.

To demonstrate the feasibility of this approach, we tracked individual cells from several different breast cancer cell lines (ER^+ MCF7, $HER2^+$ HCC1954, TNBC MDA-MB-231, subclones of those 231s, TNBC HCC1143, and the murine TNBC D2.A1 and D2.0R lines) across several different microenvironments (TCPS, protein- and peptide-coupled glass surfaces, thin layers of collagen and Matrigel, 3D Collagen and Matrigel, and in synthetic PEG-RGD gels). Our motivation for analyzing this broad set of cell lines is that they span the commonly used extrinsic subtypes of breast cancer. These subtypes are associated with specific rates and regions of recurrence.[36,37] TNBC has the highest rate of recurrence in the first five years, whereas the recurrence rate for luminal A and luminal B tumors is initially low, but remains continuous even after 10 years of follow-up [36]. Among several breast cancer subtypes, estrogen receptor positive (ER+) breast cancer is most commonly associated with bone metastasis and dormancy.[32] Although using only a small set of cell lines does not necessarily reflect the heterogeneity in these subtypes, applying the lineage tracing allowed us to observe micronenvironmental (ECM and serum) regulation of dormant states across representatives of these subtypes.

The largest drivers of variability in dormancy vs. growth in our studies were cell line source, serum, and collagen. The most obvious example is when we compared the proliferative D2A1 cells to the dormant D2.0R cells, which have obvious phenotypic differences even though derived from the same cell source. In serum, both these cells are highly proliferative, but when under serum-deprivation stress, the D2A1 cells have a bimodal population containing either proliferative or dying cells but minimal dormant cells. In contrast, the D2.0R cells shift to a population containing many dormant cells (Fig. 3). Dormancy dependent on serum was also highly cell-line dependent. While the D2 series cells were highly serum dependent, we saw minimal population shifts when we toggled serum for the HCC1954 cells across microenvironments (Figure 2), the MCF7 cells (Figure 2), nor the

MDA-MD-231 parental or cell line subclones (Figure 4). This general concept that intrinsic cell line differences determine dormancy capacity aligns with a previous study by Kloxin group, who showed that cell line subtypes showed distinct dormancy scores when they controlled for the microenvironment in a long-term 3D dormancy culture model.[16] In their synthetic matrix, ER^+ breast cancer cells underwent dormancy while triple negative breast cancer cells did not.[16]

For one cell line (HCC1954), we applied our cell lineage tracing approach across several microenvironments (2D, 3D, Collagen, Matrigel, and on collagen-derived peptides). Similar to what we observed in our prior work, the highest number of dormant cells were observed on and in collagen-rich environments.[22] The identity and dimensionality of ECM control of cell growth is well-appreciated.[38] Specifically for dormant cell behaviors, there are multiple studies that showed the degradability of materials or immobilization by environment could induce cellular dormancy.[39,40] For example, hydrogels with no adhesivity but high degradability induced cellular dormancy, while hydrogels with high adhesivity and degradability promoted growth.[39] Also, non-degradable hydrogels immobilize cells in the microenvironment, and this physical confinement can also promote dormancy.[40]

One notable limitation of our approach is that it can only quantify cellular dormancy across a population of heterogeneous cells, and not tumor dormancy. Cellular dormancy is when individual cells are quiescent and non-proliferative, and tumor dormancy is when there is an equilibrium between cell proliferation and death across the bulk of the tumor mass.[41] By individually tracking cells with bright-field microscopy in and on transparent ECMs, we can easily and reliably monitor individual cells, but cannot track individual cells once they grow enough to form small spheroids (Supplemental video S9). Also, when such spheroids grow fast enough to meet single quiescent cells nearby, such quiescent cells will no longer able to track because they merge into or overlap with the spheroids. In such cases, we cannot distinguish dormant cells from senescent cells. In our study, we monitored cellular dormancy by seeding cells at a low enough density to accurately find and track single cells, while avoiding cell clumping. Although our work here followed cells for only days, this could be extended, such as over the course of weeks. This could further improve the accuracy of distinguishing dormant vs. slowly proliferating cells. Since this method uses live microscopy, it could also be combined with live cell reporters of p38 and ERK.

We suggest this cell lineage tracing approach as a simple way to track single cell dormancy[18], and we applied it here across a variety of cell line sources and ECM environments. One of the advantages of this method is that we can trace live cells real time unlike other endpoint assays. This will help us to better understand cellular dormancy and how it is related to the tumor microenvironment of DTCs. We propose this approach has a vast array of applications, not limited to dormancy, where knowing the dynamics of a cell population with simple brightfield tracking would be beneficial. For instance, Gross *et al.* used the cell lineage tree model to capture cell cycle dynamics upon drug application, which includes drug-specific effects on cell cycle phases.[42] Combined with biomaterials expertise, this approach is powerful to explore which microenvironmental factors are critical for inducing dormancy and re-awakening cells. Given the short time frame of

these experiments, this is an excellent space in which to quickly hypothesis test regulators of dormancy and reawakening that are much faster than *in vivo* experiments. Future extensions of this work could include selecting individual cells identified via microscopy for additional profiling to understand the molecular basis of ECM-driven dormancy e.g. spatial transcriptomics.

Materials and Methods

Breast cancer cell culture

Different types of human breast cancer cell lines, including MCF7, MDA-MB-231, HCC1954, and HCC1143 were used for this study. MCF7 and MDA-MB-231 cells were cultured under 5% CO2 and 37°C with DMEM containing 10% fetal bovine serum (FBS) and 1% penicillin/streptomycin (pen/strep). MDA-MB-231 cell subclones were generated by Ning-Hsuan Tseng,[33] and the same culturing method was used as the parental MDA-MB-231 cell line. HCC1954 and HCC1143 were cultured under 5% CO2 and 37°C with RPMI containing 10% FBS and 1% pen/strep. Two different types of mouse mammary tumor cells were also used, which were derived from spontaneous mouse mammary tumors, originated from D2 hyperplastic alveolar nodule in Miller lab.[43,44] D2A1 (proliferative) and D2.0R (dormant) cells were cultured under 5% CO2 and 37°C with DMEM containing 10% FBS and 1% pen/strep.

Live cell microscopy for tracing individual cells

Cells were seeded on TCPS, functionalized glass coverslips, 2D collagen gel, 2D Matrigel, or in 3D collagen gel or 3D Matrigel. The cell culture media was changed 24 hours after cell seeding, to either normal growth medium (with 10% FBS) or serum free medium. Six hours after the media change, time-lapse images of single cells were taken for 50 hours, at either 15-minute (for 2D experiments) or 30-minute intervals (for 3D experiments). Imaging was performed using Zeiss Axio Observer Z1 Inverted Fluorescence Microscope.

Preparation of culturing environment and cell seeding for 2D environment

For tissue culture polystyrene (TCPS): After at least 80% confluence achieved in T-25 flasks, we harvested cells for seeding on different substrates with varying media conditions. Used approximately 2mL of 1X phosphate buffered saline (PBS) to wash the flask before using 2mL trypsin for 2-5 minutes to cleave cells off flask surface. Then we deactivated trypsin with 4mL of regular media. Placed the gathered liquid and cells in a 10mL conical tube in a centrifuge for 5 minutes at 200G. Aspirated the cell pellet by vacuuming the supernatant and resuspend the cells in 1mL of media. Counted the cells using an automated cell counter (a hemocytometer has been used with near similar results) and mathematically calculated the volume needed to seed approximately 1000 cells in a 24-well plate. Used similar ratios for greater-numbered plates by dividing the cells with the surface area given by Thermo Fischer and other companies. After seeding, we waited 24 hours for cells to adhere before changing media conditions (serum free DMEM and RPMI media). After the media change, we waited an additional 6 hours before beginning imaging for 50 hours.

For 2D Matrigel: We thawed Matrigel (Corning) overnight in the 4-°C fridge to prepare for use the following day. 80% confluence was achieved in T-25 flasks, harvested the cells to use with different growing medium on top of the Matrigel. Once completely sterilized, 100μL Matrigel was slowly pipetted into a warm 96-well plate; then was placed to polymerize in the 37°C incubator for 20 minutes. While waiting for the Matrigel to solidify, the same cell harvesting procedure as described in TCPS method was used. Calculated a 200-cell density in each well placed in 100μL of media to seed on top of the Matrigel layer. Waited 24 hours for cells to adhere before changing media conditions and imaging (Fig. 1c).

For 2D collagen gel: Rat tail collagen I was taken out of 4°C fridge and kept on ice. 410μL of rat tail collagen I solution at 3mg/mL was mixed with 520μL of serum free media and 25μL of sterile filtered 1M NaOH in microcentrifuge tubes, final concentration of which is 1.3mg/mL. 100μL of this mixture solution was taken and placed into a pre-warmed 96-well plate, then was placed to polymerize in the 37°C insulator for 30 minutes. While waiting for the collagen gels to polymerize, the same cell harvesting procedure as described in TCPS method was used. 200 cells per well were seeded on top of each 2D collagen gel in a 96-well plate, and 100μL of media was placed on top. We waited 24 hours before changing media with or without serum and imaging (Supplemental video S10).

For 2D functionalized coverslips: Rat tail collagen I protein and collagen I integrin-binding peptide were immobilized on glass coverslips. Briefly, 15mm coverslips were oxygen plasma treated (Harrick Plasma, Ithaca, NY, USA), and silanized through vapor phase deposition of (3-aminopropyl)triethoxysilane (Sigma-Aldrich) at 90°C for a minimum of 18 hours. The coverslips were sequentially rinsed in toluene (Fischer Scientific), 95% ethanol (Decon Laboratories, King of Prussia, PA, USA), and water, and dried at 90°C for one hour. These were subsequently functionalized with 10 g/L N,N,-disuccinimidyl carbonate (Sigma-Aldrich) and 5% v/v diisopropylethylamine (Sigma-Aldrich) in acetone (Fischer Scientific) for two hours. Finally, coverslips were rinsed three times in acetone and air-dried for 10 minutes. Rat tail collagen I protein and collagen I integrin-binding peptide were then covalently bound to the glass coverslips via the reactive amines at 2 μg/cm^2 concentration. The peptide sequence CGPGPPGPPGPPGPPGPPGFOGERGPPGPPGPPGPPGPP (GFOGER) was used as the collagen I binding peptide. The rat tail collagen I protein and GFOGER peptide peptide were subsequently blocked using methyl-PEG24-amine (MA-PEG24) (Thermo Fisher Scientific). Post functionalization, the coverslips were UV sterilized for minimum of 1 hour. The cells were then added on the coverslips. In prior trials, we noted that the cells adhered less to coverslips, thus we seeded a higher amount of cells (4000 cells per well in a 24-well plate) compared to 1000 cells on plastic, so that the cell numbers during analysis were comparable amounts between the two substrates. The cells were allowed to adhere on the surface before changing the media and imaging (Fig. 1d).

Preparation of culturing environment and cell seeding for 3D environment

For 3D Matrigel: We thawed Matrigel overnight in the 4°C fridge and placed the Matrigel on ice on the day of experiment. For all the cell lines except for D2 series cells and MDA-MB-231 cells, 5000 cells were mixed with 10μL of Matrigel, and the 10μL of Matrigel was

placed on a pre-warmed 24-well plate, and the plate was put in the 37°C incubator for 20 minutes to fully polymerize Matrigel. Once it gets polymerized, 1mL of media was put in each well. D2 series cells and MDA-MB-231 cells were seeded at 1000 cells per 10uL gel as they grow faster than others, so we put fewer cells to make cells sparse enough for analysis.

For 3D collagen gel: Rat tail collagen I was taken out of 4°C fridge and kept on ice. 41μL of rat tail collagen I solution at 3mg/mL was mixed with 52μL of serum free media and 2.5μL of sterile filtered 1M NaOH in microcentrifuge tubes, final concentration of which is 1.3mg/mL. 90μL of this mixture solution was taken out to resuspend cell pellets of 45000 cells for 9 collagen gels. 10μL of this solution was used to make one collagen gel with 5000 cells per gel in a 24-well plate for all cell lines except for D2 series cells and MDA-MB-231 cells. Once it gets polymerized, 1mL of media was put in each well. D2 series cells and MDA-MB-231 cells were seeded at 1000 cells per 10uL gel as they grow faster than others, so we put fewer cells to make cells sparse enough for analysis.

For 3D PEG-RGD gel: 20kDa 4-arm PEG-maleimide (JenKem Technology) was dissolved in serum free media at pH7.4 at 20 wt%, mixed with 2mM RGD peptide (peptide sequence: GRGDSPCG) purchased from GenScript, and we let them react at room temperature for 10 minutes. RGD peptides were used as integrin binding peptides. 1.5kDa PEG-dithiol (JenKem Technology) was dissolved in 1X PBS at pH 7.4. The weight of PEG-dithiol was calculated to have 1:1 molar ratio of thiol to maleimide when mixed together. PEG-dithiol solution was mixed with 25 mol% of MMP-degradable peptide, GCRDGPQGIWGQDRCG, purchased from GenScript for the PEG-RGD gels with degradable sites. 1μL of PEG-dithiol solution was placed first in the middle of the well on a 24-well plate, followed by an addition of 9μL of PEG-maleimide solution with peptides and cells on top of the 1μL PEG-dithiol solution. 10,000 cells per gel was seeded in each 10μL gel, and 1mL of media was put in the 24-well plate after letting the gels to fully polymerize for 5-10 minutes in the 37°C incubator. 24 hours after gelation, the culture media was changed to serum-containing or serum-free media, followed by 50-hour imaging for cell lineage tree analysis (Supplemental video S11).

Lineage Tree Analysis

After the 50-hour imaging was done in the Zeiss Axio Observer Z1 Inverted Fluorescence Microscope, all the microscope image files were transferred to open in Imaris software. Microscope files were then converted to movie files showing a timeline as seen in the videos of each cell population (dividing, dying, quiescent) (Supplemental videos S5–8). We manually marked specific time points when a cell divides or dies on an Excel spreadsheet for randomly selected cells for each condition, and generated cell lineage trees to illustrate individual cell growth.

As seen in Fig. 1a, each horizontal line indicates a single cell during the multi-hour time-lapse microscopy imaging. When a cell divides, the horizontal line diverges at that time point. When a cell dies, it is marked with a red “x” at the end. Single horizontal lines that do not diverge throughout the whole time of imaging, mean that these cells did not divide but are still alive for the entire period of time-lapse microscopy imaging.

From each cell lineage tree, we counted the numbers of non-dividing and dying cells, as well as the number of cells that divide once or that divide two or more times during the 50-hour imaging. We created stacked bar graphs in Prism software, visualizing the proportion of cells in each category (no division; cell death; 1 cell division; ≥2 cell division) (Fig. 1c).

Immunofluorescence staining and imaging

After the 50-hour imaging is finished, cells were fixed with 10% formalin. Cells were then permeabilized and stained with DAPI, Ki-67 (ab156956, Abcam), ERK (ab54230, Abcam), and p38 (#4511, CellSignaling). IF stained cells were imaged using Zeiss Cell Observer SD Spinning Disc Confocal Microscope.

Statistical analysis

Two-sided Fisher exact test was performed to determine whether the association between the categories (dormant versus non-dormant cells) is significant under various conditions. The open source Scipy library from Python 3.9 was used to calculate the p-value.

Supplementary Material

Refer to Web version on PubMed Central for supplementary material.

Acknowledgements

The authors would like to thank Sean Gross for helping with learning the cell lineage tracing approach. The authors would also like to thank Ning-Hsuan Tseng for providing the cell subclones of MDA-MB-231 cell line. This work was supported by a grant from the Jayne Koskinas Ted Giovanis Foundation for Health and Policy, an NSF CAREER grant (DMR-1454806), and grants from the NIH (R21 CA223783, DP2 CA186573, and U01 CA265709) to S.R.P. S.R.P. was supported by an Armstrong Professorship at UMass Amherst. This work was also supported by a grant from the NIH (U01-CA215709) to A.S.M, and a grant from the NIH (U54-CA209988) to L.M.H.

References

[1]. Torre LA, Islami F, Siegel RL, Ward EM, Jemal A, Cancer Epidemiol Biomarkers Prev 2017, 26, 444. [PubMed: 28223433]

[2]. Sung H, Ferlay J, Siegel RL, Laversanne M, Soerjomataram I, Jemal A, Bray F, CA Cancer J Clin 2021, 71, 209. [PubMed: 33538338]

[3]. Allemani C, Weir HK, Carreira H, Harewood R, Spika D, Wang X-S, Bannon F, v Ahn J, Johnson CJ, Bonaventure A, et al., Lancet 2015, 385, 977. [PubMed: 25467588]

[4]. Allemani C, Matsuda T, di Carlo V, Harewood R, Matz M, Nikšić M, Bonaventure A, Valkov M, Johnson CJ, Estève J, et al., Lancet 2018, 391, 1023. [PubMed: 29395269]

[5]. Anyigba CA, Awandare GA, Paemka L, Exp Biol Med 2021, 246, 1377.

[6]. Weiss A, Chavez-MacGregor M, Lichtensztajn DY, Yi M, Tadros A, Hortobagyi GN, Giordano SH, Hunt KK, Mittendorf EA, JAMA Oncol 2018, 4, 203. [PubMed: 29222540]

[7]. K. C (eds). Howlader N, Noone AM, Krapcho M, Miller D, Bishop K, Altekruse SF, Kosary CL, Yu M, Ruhl J, Tatalovich Z, Mariotto A, Lewis DR, Chen HS, Feuer EJ, National Cancer Institute; Cancer Statistics Review 2021, 1992.

[8]. Seyfried TN, Huysentruyt LC, Crit Rev Oncog 2013, 18, 43. [PubMed: 23237552]

[9]. Sosnoski DM, Norgard RJ, Grove CD, Foster SJ, Mastro AM, Clin Exp Metastasis 2015, 32, 335. [PubMed: 25749879]

[10]. Shupp AB, Kolb AD, Mukhopadhyay D, Bussard KM, Cancers (Basel) 2018, 10, DOI 10.3390/cancers10060182.

[11]. Carlson P, Dasgupta A, Grzelak CA, Kim J, Barrett A, Coleman IM, Shor RE, Goddard ET, Dai J, Schweitzer EM, et al., Nat Cell Biol 2019, 21, 238. [PubMed: 30664790]

[12]. Endo H, Inoue M, Cancer Sci 2019, 110, 474. [PubMed: 30575231]

[13]. Ghajar CM, Peinado H, Mori H, Matei IR, Evason KJ, Brazier H, Almeida D, Koller A, Hajjar KA, Stainier DYR, et al., Nat Cell Biol 2013, 15, 807. [PubMed: 23728425]

[14]. Malladi S, Macalinao DG, Jin X, He L, Basnet H, Zou Y, de Stanchina E, Massague J, Cell 2016, 165, 45. [PubMed: 27015306]

[15]. Micalet A, Moeendarbary E, Cheema U, ACS Biomater Sci Eng 2021, DOI 10.1021/acsbiomaterials.0c01530.

[16]. Ovadia EM, Pradhan L, Sawicki LA, Cowart JE, Huber RE, Polson SW, Chen C, van Golen KL, Ross KE, Wu CH, et al., Adv Biosyst 2020, 4, 2000119.

[17]. Pradhan S, Slater JH, Biomaterials 2019, 215, 119177. [PubMed: 31176804]

[18]. Mohammadi F, Visagan S, Gross SM, Karginov L, Lagarde JC, Heiser LM, Meyer AS, bioRxiv 2021, 2021.06.25.449922.

[19]. Stepanenko AA, v Dmitrenko V, Gene 2015, 574, 193. [PubMed: 26260013]

[20]. Barney LE, Dandley EC, Jansen LE, Reich NG, Mercurio AM, Peyton SR, Integr Biol (Camb) 2015, 7, 198. [PubMed: 25537447]

[21]. Brooks EA, Jansen LE, Gencoglu MF, Yurkevicz AM, Peyton SR, ACS Biomater Sci Eng 2018, 4, 707. [PubMed: 33418758]

[22]. Barney LE, Hall CL, Schwartz AD, Parks AN, Sparages C, Galarza S, Platt MO, Mercurio AM, Peyton SR, Sci Adv 2020, 6, eaaz4157. [PubMed: 32195352]

[23]. Rijal G, Li W, Biomaterials 2016, 81, 135. [PubMed: 26731577]

[24]. Edmondson R, Adcock AF, Yang L, PLoS One 2016, 11, e0158116. [PubMed: 27352049]

[25]. Josan C, Kakar S, Raha S, Adipocyte 2021, 10, 361. [PubMed: 34288778]

[26]. Naumov GN, MacDonald IC, Weinmeister PM, Kerkvliet N, v Nadkarni K, Wilson SM, Morris VL, Groom AC, Chambers AF, Cancer Res 2002, 62, 2162. [PubMed: 11929839]

[27]. Naumov GN, Townson JL, MacDonald IC, Wilson SM, Bramwell VHC, Groom AC, Chambers AF, Breast Cancer Res Treat 2003, 82, 199. [PubMed: 14703067]

[28]. Morris VL, Tuck AB, Wilson SM, Percy D, Chambers AF, Clin Exp Metastasis 1993, 11, 103. [PubMed: 8422701]

[29]. Morris VL, Koop S, MacDonald IC, Schmidt EE, Grattan M, Percy D, Chambers AF, Groom AC, Clin Exp Metastasis 1994, 12, 357. [PubMed: 7923988]

[30]. Fares J, Fares MY, Khachfe HH, Salhab HA, Fares Y, Signal Transduct Target Ther 2020, 5, 28. [PubMed: 32296047]

[31]. Gomis RR, Gawrzak S, Mol Oncol 2017, 11, 62. [PubMed: 28017284]

[32]. Coleman RE, Rubens RD, Br J Cancer 1987, 55, 61. [PubMed: 3814476]

[33]. Tseng N-H, EXTRACELLULAR MATRIX STIFFNESS AS A CUE TO SHAPE PHENOTYPIC EVOLUTION OF TRIPLE NEGATIVE BREAST CANCER, University of Massachusetts Amherst, 2022. 10.7275/28638785

[34]. Gay LJ, Malanchi I, Biochim Biophys Acta Rev Cancer 2017, 1868, 231. [PubMed: 28501561]

[35]. Sosa MS, Bragado P, Aguirre-Ghiso JA, Nat Rev Cancer 2014, 14, 611. [PubMed: 25118602]

[36]. Ignatov A, Eggemann H, Burger E, Ignatov T, J Cancer Res Clin Oncol 2018, 144, 1347. [PubMed: 29675790]

[37]. Yerushalmi R, Woods R, Kennecke H, Speers C, Knowling M, Gelmon K, Breast Cancer Res Treat 2010, 120, 753. [PubMed: 19701704]

[38]. Ruud KF, Hiscox WC, Yu I, Chen RK, Li W, Breast Cancer Research 2020, 22, 82. [PubMed: 32736579]

[39]. Farino Reyes CJ, Pradhan S, Slater JH, Adv Healthc Mater 2021, 10, 2002227.

[40]. Preciado JA, Reátegui E, Azarin SM, Lou E, Aksan A, Technology (Singap World Sci) 2017, 05, 129.

[41]. Dittmer J, Semin Cancer Biol 2017, 44, 72. [PubMed: 28344165]

[42]. Gross SM, Mohammadi F, Sanchez-Aguila C, Zhan PJ, Meyer AS, Heiser LM, bioRxiv 2021, 2020.07.24.219907.

[43]. Miller FR, McEachern D, Miller BE, Cancer Res 1989, 49, 6091. [PubMed: 2790822]

[44]. Rak JW, McEachern D, Miller FR, Br J Cancer 1992, 65, 641. [PubMed: 1586590]

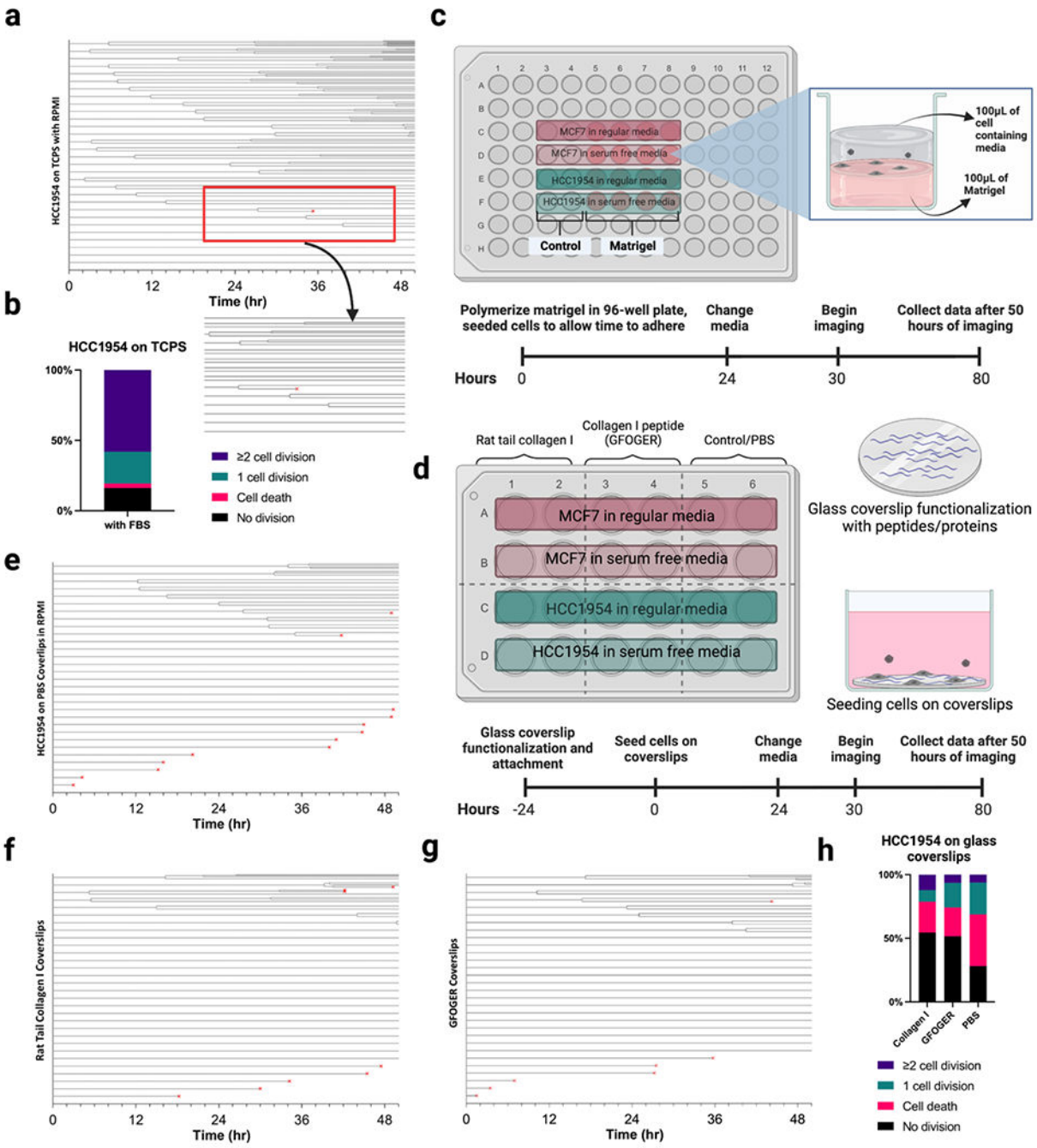

Fig. 1. Experimental setups and timelines for 2D environments.

(**a**). Shows a cell lineage tree of HCC1954 cells on TCPS obtained by randomly tracking 30 individual cell proliferation across 50 hours. Each time a cell splits, it is denoted in the graph by splitting into two lines. Increasing on the y-axis shows least proliferating to most. If a cell doesn't split, it will have a straight line across the entire graph. When encountering a dying cell, the time of death is marked with a red 'x'. (**b**). Bar graph distribution of cell division and death from the lineage analysis. (**c**). This schematic consists of the seeding procedure and experimental timeline of two cell lines (MCF7 and HCC1954) in different

media conditions on top of 2D Matrigel in a 96-well plate. (**d**). Schematic of a 24-well plate containing protein treated coverslip conditions with an included timeline. (**e-g**). Cell lineage analyses of HCC1954 in serum containing media (RPMI) across the coverslip conditions: (**e**). PBS-treated coverslip, (**f**). Collagen I protein treated coverslip, and (**g**). Collagen I peptide (GFOGER) treated coverslip. (**h**). Stacked bar graph for coverslip conditions from figures e-g.

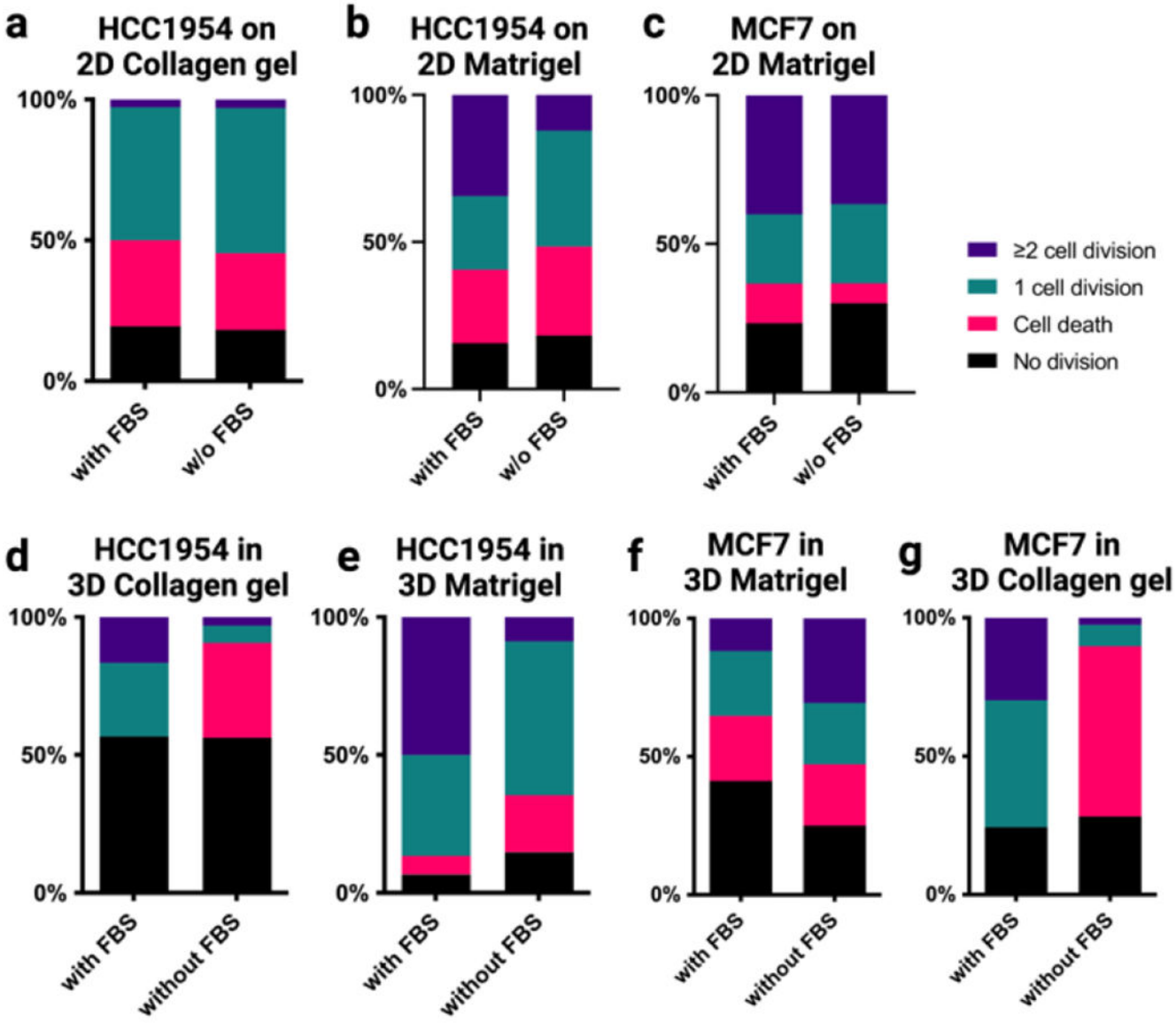

Fig. 2. Distribution of cell proliferation in 2D and 3D gel environments.

(**a**) The stacked bar graph showing proportion of cells with 0, 1, 2+ cell divisions or with cell death, which data was taken from the cell lineage analysis conducted on HCC1954 cells seeded on 2D collagen gel in regular RPMI. (**b-c**). Bar graph showing proportion of cells with 0, 1, 2+ cell divisions or with cell death for (**b**) HCC1954 and (**c**) MCF7 cells on 2D Matrigel. (**d**). Bar graph showing proportion of cells with 0, 1, 2+ cell divisions or with cell death for HCC1954 cells in 3D collagen gel. (**e**). Bar graph showing proportion of cells with 0, 1, 2+ cell divisions or with cell death for HCC1954 in 3D Matrigel. (**f**). Stacked bar graphs showing proportion of cell populations with 0, 1, 2+ cell divisions or with cell death for MCF7 in 3D Matrigel. (**g**). Stacked bar graphs showing proportion of cell populations with 0, 1, 2+ cell divisions or with cell death for MCF7 in 3D collagen gel.

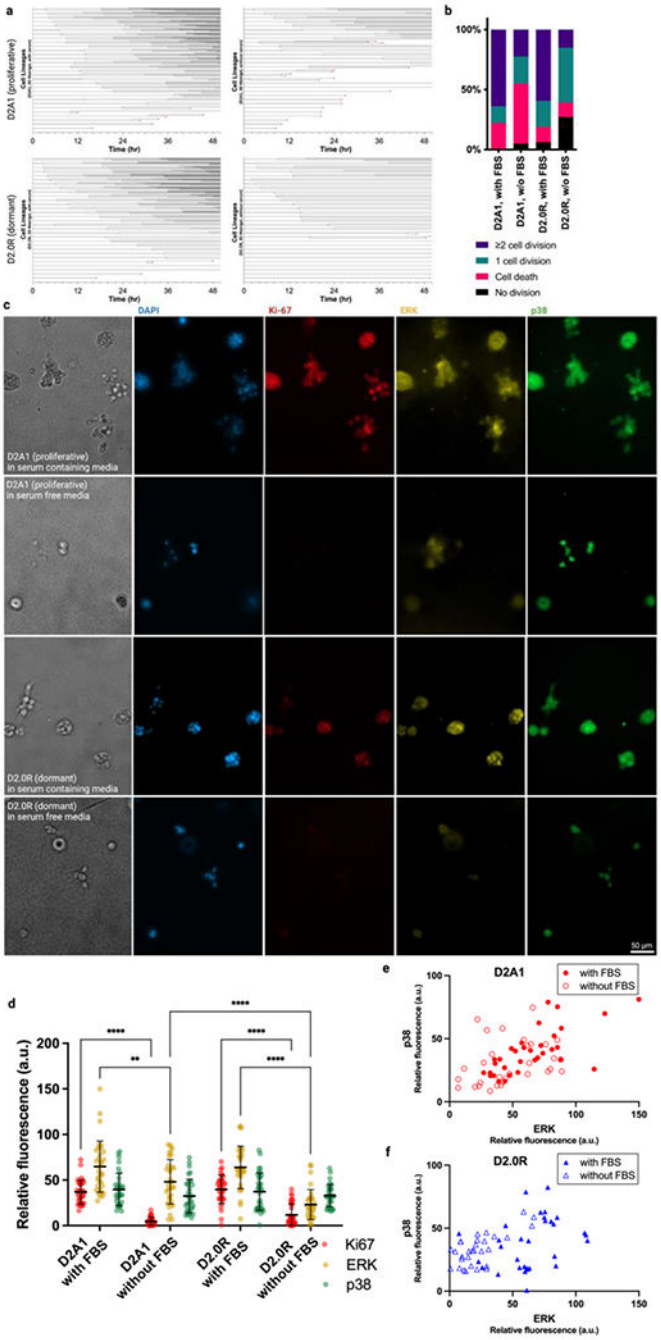

Fig. 3. Mouse breast cancer cells that have proliferative (D2A1) or dormant (D2.0R) phenotype in 3D Matrigel.

(**a**). Cell lineage trees of D2A1 (proliferative) and D2.0R (dormant) cells in serum containing and serum free conditions. Top row is showing D2A1 lineages, and bottom row is showing D2.0R lineages. Left column is the lineage trees of cells under serum containing condition, and right column is the lineage trees of cells under serum free condition. (**b**). A stacked bar graph showing proportion of cells with 0, 1, 2+ cell divisions or with cell death of D2 series cells, and the number of each group was calculated from the cell lineage trees

shown in (a). (**c**). IF staining images of D2 series cells in serum-containing and serum-free conditions. Images on the far-left column are brightfield images, and the images from 2nd to 5th columns are IF staining images. Cells were stained with DAPI (blue), Ki-67 (red), ERK (yellow), and p38 (green). Scale bar = 50μm. **(d)**. Quantification of fluorescent levels of Ki-67, ERK, and p38 in each condition. **(e-f)**. Scattered plot of ERK and p38 expression levels in individual cells of (e) D2A1 and (f) D2.0R. Each dot indicates data from a single cell.

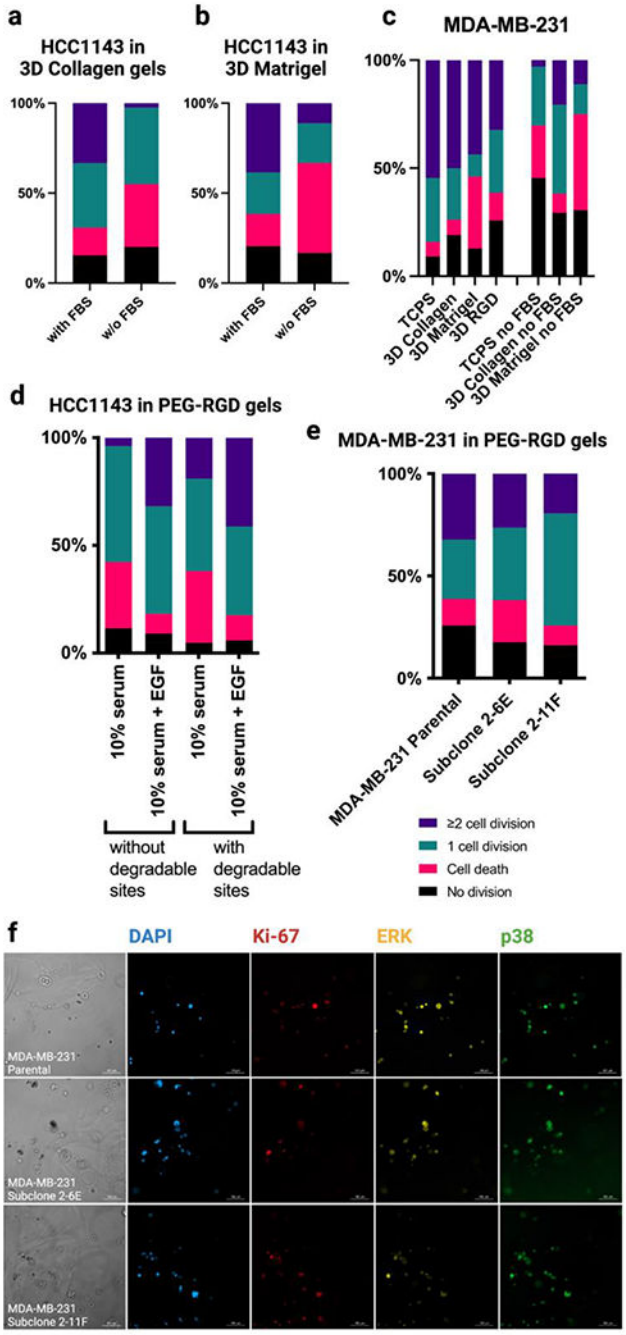

Fig. 4. Triple negative breast cancer lines in PEG-RGD gels.

(**a-b**). Stacked bar graphs from the cell lineage analysis conducted on HCC1143 cells in (a) 3D Collagen and (b) 3D Matrigel. (**c**). Stacked bar graphs from cell lineage analysis of MDA-MB-231 on TCPS and in various 3D environments. Four columns on the left are with FBS, and three columns on the right are without FBS. (**d**) A stacked bar graph from the cell lineage analysis conducted on HCC1143 cells in a 3D PEG-RGD system with different serum and EGF conditions (**e**). Bar graph of the MDA-MB-231 cell line with its subclones 2-6E and 2-11F in 3D PEG-RGD gels. (**f**). IF-stained images of MDA-MB-231 parental and

subclones in 3D PEG-RGD gels with FBS. DAPI is shown in blue, Ki-67 in red, ERK in yellow, p38 in green. Scale bar = 100μm.

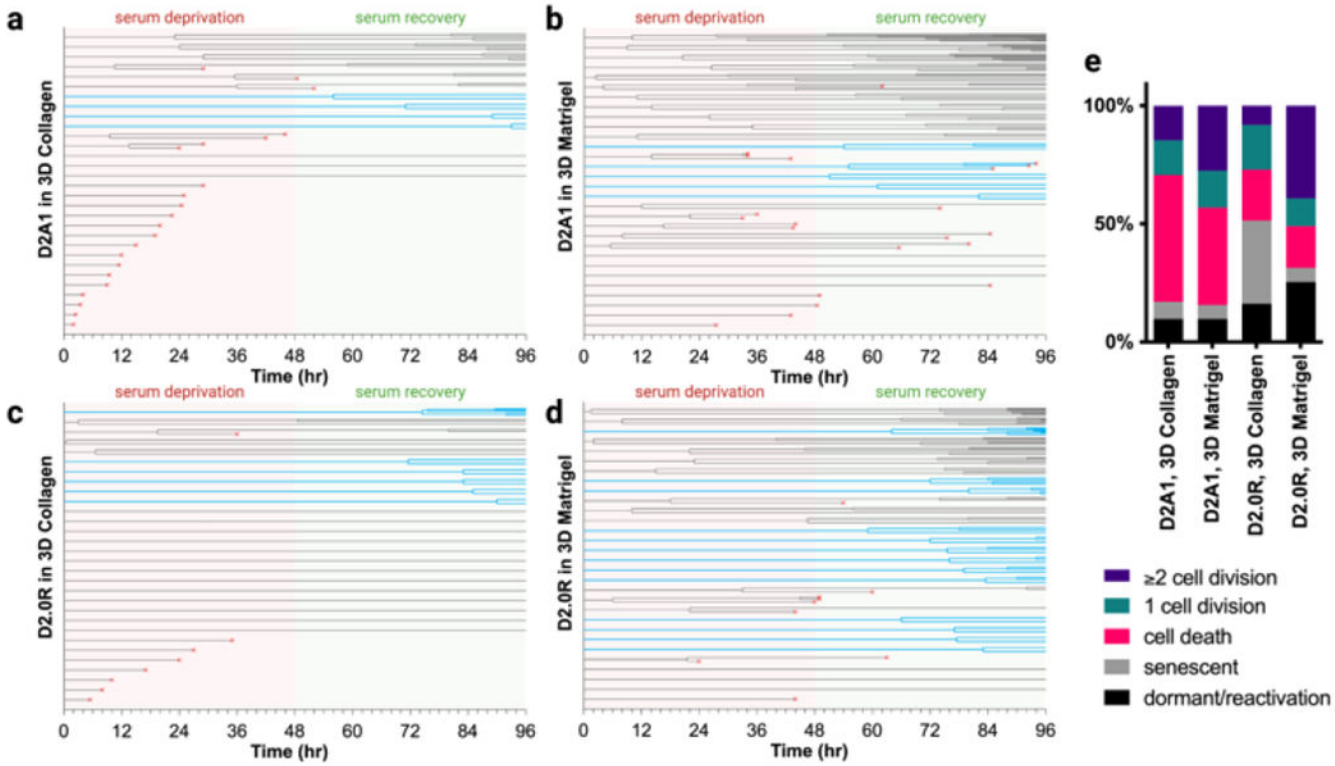

Fig. 5. Cell lineage tracing of D2 series cells in 3D collagen and Matrigel during serum recovery. (**a-d**). Cell lineage analysis for (a) D2A1 in 3D collagen, (b) D2A1 in 3D Matrigel, (c) D2.0R in 3D collagen, and (d) D2.0R in 3D Matrigel. Imaging started from Time=0hr in the graphs, which was 6 hours after serum deprivation started. 48 hours after imaging cells under serum deprivation, we placed full serum media (10% FBS) and continued imaging for additional 48 hours. Blue horizontal lines indicate the cells showed proliferation during the 48-hour serum recovery window. (**e**). Stacked bar graphs showing the distribution of each cell population, such as dormant/reactivation, senescent, cell death, 1 cell division, and 2 or more cell divisions during 96-hour tracing.